Journal of Developing Drugs
ISSN: 2329-6631

Trivedi et al., J Develop Drugs 2015, 4:3
DOI: 10.4172/2329-6631.1000133

Research Article Open Access

Characterization of Physical, Thermal and Spectral Properties of Biofield Treated 2, 6-Diaminopyridine

Mahendra Kumar Trivedi[1], Rama Mohan Tallapragada[1], Alice Branton[1], Dahryn Trivedi[1], Gopal Nayak[2], Rakesh Kumar Mishra[2] and Snehasis Jana[2*]

[1]*Trivedi Global Inc., 10624 S Eastern Avenue Suite A-969, Henderson, NV 89052, USA*
[2]*Trivedi Science Research Laboratory Pvt. Ltd., Hall-A, Chinar Mega Mall, Chinar Fortune City, Hoshangabad Rd., Bhopal, Madhya Pradesh, India*

Abstract

2, 6-Diaminopyridine (2, 6-DAP) has extensive use in synthesis of pharmaceutical compounds. The objective of present research was to investigate the influence of biofield treatment on physical, thermal and spectral properties of 2, 6-DAP. The study was performed in two groups, control and treated. The control group remained as untreated, and biofield treatment was given to treatment group. The control and treated 2, 6-DAP samples were characterized by X-ray diffraction (XRD), Differential scanning calorimetry (DSC), Thermo gravimetric analysis (TGA), Laser particle size analyzer, surface area analyzer**,** Fourier transform infrared (FT-IR) spectroscopy, and UV-visible spectroscopy. XRD analysis revealed decrease in intensity of the peaks of treated 2, 6-DAP with respect to control. Unit cell volume and molecular weight were decreased by 2.97% and 2.98% respectively in treated 2, 6-DAP as compared to control. Crystallite size was decreased by 24.70% in treated 2, 6-DAP with respect to control. DSC analysis showed no significant change in melting temperature of treated 2, 6-DAP with respect to control. Nevertheless, the treated 2, 6-DAP showed significant increase in latent heat of fusion by 35.52% as compared to control 2, 6-DAP. TGA analysis showed decrease in percent weight loss of the treated 2, 6-DAP in comparison with control. Additionally, substantial increase in maximum thermal decomposition temperature (T_{max}) was observed in treated 2, 6-DAP (203.52°C) as compared with control 2, 6-DAP (186.84°C). Particle size analysis results showed a substantial decrease in d_{50} (average particle size) and d_{99} (size exhibited by 99% of the particles) of the treated 2, 6-DAP by 20.5 and 57.4%, respectively as compared to control. Additionally, the BET analysis showed substantial increase in surface area of treated 2, 6-DAP by 75.58% as compared to control. FT-IR spectrum of treated 2, 6-DAP showed alteration in O-H stretching (3390→3370 cm^{-1}), C-H stretching (3132→3138 cm^{-1}) and N-H bending (1637→1604 cm^{-1}) vibration peaks with respect to control. However, UV-visible analysis of treated 2, 6-DAP showed no significant changes in absorption peaks (λ_{max}) with respect to control. Overall, the results demonstrated that biofield has significant impact on the physical, thermal and spectral properties of the treated 2, 6-DAP.

Keywords: Biofield treatment; X-ray diffraction; Differential scanning calorimetry; Thermo gravimetric analysis; Laser particle size analyzer; Surface area analyzer**;** Fourier transform infrared (FT-IR) spectroscopy

Abbreviation

2, 6-DAP: 2, 6- Diaminopyridine; XRD: X-ray diffraction; DSC: Differential scanning calorimetry; TGA: Thermo gravimetric analysis; DTA: Differential thermal analysis; DTG: Derivative thermo gravimetry; FT-IR: Fourier transforms infrared

Introduction

Diaminopyridine are important class of organic compounds, mostly used for synthesis of dyes, cosmetics, drugs and explosives. Recently, 2, 4-diaminopyridine was used as pharmacological agent for muscle relaxant used in anesthesia and it can increase the neuromuscular transmission in certain disease conditions. Additionally, 3, 4-diaminopyridine was used as a drug for the treatment of Lambert–Eaton syndrome (a rare autoimmune disorder characterized by muscle weakness) and also prescribed for multiple sclerosis [1]. Moreover, 4-aminopyridine a pyridine derivative was used for K-channel blocker in axonal membranes, and also to prolong the nerve action potential [2]. 2, 6- Diaminopyridine (2, 6-DAP) is used for synthesis of hair dye and energetic compounds [3]. Besides, it is also used as intermediate for the synthesis of epoxy curing agent, polyamides, and preparation of analgesic phenazo- pyridine hydrochloride. Further, it was reported that amino pyridine and diaminopyridine are present in many biologically significant molecules such as folate, antifolate drugs, and cytosine derivatives [4]. However, it has been shown that 2, 6-DAP and related compounds have less water solubility and it does not cross the blood brain barrier [5], which limits its pharmaceutical applications. Hence, alternative strategies should be devised in order to improve the solubility and stability of the compounds. Mohammadi et al. used fast neutron and gamma irradiation to investigate the thermal, structural and colorant properties of 2, 6-DAP [6]. Recently biofield treatment has been reported to use as an effective alternative strategy for altering the physical and thermal properties of various metals and ceramics [7-10]. Hence, by considering the pharmaceutical significance of 2, 6-DAP, the present study was aimed to evaluate the influence of biofield treatment on physical, thermal and spectral properties of this compound.

German physicist George Christopher Lichtenberg coined the term Bioelectrography in 1770 and it was observed that light coming out from different subjects in electrical fields [11]. Moreover, short-lived electrical events called action potential exist in several types of animal cells, neuronal cells, muscle cells, and endocrine cells. For

***Corresponding author:** Snehasis Jana, Trivedi Science Research Laboratory Pvt. Ltd., Hall-A, Chinar Mega Mall, Chinar Fortune City, Hoshangabad Rd., Bhopal- 462026, Madhya Pradesh, India, Tel: +91-755-6660006; E-mail: publication@trivedisrl.com

Received August 13, 2015; **Accepted** August 24, 2015; **Published** August 28, 2015

Citation: Trivedi MK, Tallapragada RM, Branton A, Trivedi D, Nayak G, et al. (2015) Characterization of Physical, Thermal and Spectral Properties of Biofield Treated 2, 6-Diaminopyridine. J Develop Drugs 4: 133. doi:10.4172/2329-6631.1000133

instance, neurons which are present in human nervous system have the ability to transmit the information in the form of electrical signals [12-16]. Additionally, the biofield is a cumulative outcome of electric and magnetic field, exerted by the human body [17,18]. It is generates through some internal dynamic processes such as blood flow, lymph flow, brain functions, and heart function in the human body.

Thus, human beings have the ability to harness the energy from environment/Universe and can transmit into any object (living or non-living) around the Globe. The object(s) always receive the energy and responding into a useful manner that is called biofield energy. Mr. Trivedi's unique biofield treatment is also known as The Trivedi Effect®. Mr. Trivedi is known to transform the characteristics of various living and nonliving things. The biofield treatment has improved the growth and production of agriculture crops [19-22] and significantly altered the phenotypic characteristics of various pathogenic microbes [23-25]. Additionally, biofield treatment has substantially altered the medicinal, growth and anatomical properties of ashwagandha [26]. After considering the above mentioned outcome from biofield treatment and pharmaceutical applications of 2, 6-DAP, this work was undertaken to investigate the impact on physical, thermal and spectral properties of the 2, 6-DAP.

Materials and Methods

2, 6-Diaminopyridine (2, 6-DAP) was procured from SD Fine Chemicals Limited, India. The control and treated samples were characterized by XRD, DSC, TGA, laser particle size analyzer, surface area analyzer, FT-IR and UV visible analysis.

Biofield treatment

2, 6-Diaminopyridine (2, 6-DAP) was divided into two parts; one was kept as a control sample, while the other was subjected to Mr. Trivedi's biofield treatment and coded as treated sample. The treatment group was in sealed pack and handed over to Mr. Trivedi for biofield treatment under laboratory condition. Mr. Trivedi provided the treatment through his energy transmission process to the treated group without touching the sample. After biofield treatment the control and treated group was subjected to physicochemical characterization under standard laboratory conditions.

Characterizations

X-ray diffraction (XRD) study

XRD analysis of control and treated 2, 6-DAP was carried out on Phillips, Holland PW 1710 X-ray diffract meter system, which had a copper anode with nickel filter. The radiation of wavelength used by the XRD system was 1.54056 Å. The data obtained from this XRD were in the form of a chart of 2θ vs. intensity and a detailed table containing peak intensity counts, d value (Å), peak width (θ°), relative intensity (%) etc. The crystallite size (G) was calculated by using formula:

$G=k\lambda/(b\cos\theta)$

Here, λ is the wavelength of radiation used, b is full width half-maximum (FWHM) of peaks and k is the equipment constant (=0.94). Percentage change in crystallite size was calculated using following formula:

Percentage change in crystallite size$=[(G_t - G_c) / G_c] \times 100$

Where, G_c and G_t are crystallite size of control and treated powder samples respectively.

Differential scanning calorimetry (DSC)

DSC was used to investigate the melting temperature and latent heat of fusion (ΔH) of samples. The control and treated 2, 6-DAP samples were analyzed using a Pyris-6 Perkin Elmer DSC on a heating rate of 10°C/min under air atmosphere and air was flushed at a flow rate of 5 mL/min.

Percentage change in latent heat of fusion was calculated using following equations:

$$\% \text{ change in Latent heat of fusion} = \frac{[\Delta H_{Treated} - \Delta H_{Control}]}{\ddot{A}H_{Control}} \times 100$$

Where, $\Delta H_{Control}$ and $\Delta H_{Treated}$ are the latent heat of fusion of control and treated samples, respectively.

Thermo gravimetric analysis-differential thermal analysis (TGA-DTA)

Thermal stability of control and treated 2, 6-DAP were analyzed by using Mettler Toledo simultaneous TGA and Differential thermal analyzer (DTA). The samples were heated from room temperature to 400°C with a heating rate of 5°C/min under air atmosphere.

Particle size analysis

The average particle size and particle size distribution were analyzed by using Sympetac Helos-BF laser particle size analyzer with a detection range of 0.1 micrometer to 875 μm. Average particle size d_{50} and d_{99} (size exhibited by 99% of powder particles) were computed from laser diffraction data table. The d_{50} and d_{99} values were calculated by the following formula:

Percentage change in d_{50} size=100 × (d_{50} treated- d_{50} control)/d_{50} control

Percentage change in d_{99} size=100× (d_{99} treated- d_{99} control)/d_{99} control

Surface area analysis

Surface area of 2, 6-DAP were characterized by surface area analyzer, SMART SORB 90 Brunauer-Emmett-Teller (BET) using ASTM D 5604 method which had a detection range of 0.2-1000 m^2/g. Percent changes in surface area were calculated using following equation:

$$\% \text{ change in surface area} = \frac{[S_{Treated} - S_{Control}]}{S_{Control}} \times 100$$

Where, $S_{Control}$ and $S_{Treated}$ are the surface area of control and treated samples respectively.

FT-IR spectroscopy

FT-IR spectra were recorded on Shimadzu's Fourier transform infrared spectrometer (Japan) with frequency range of 4000-500 cm^{-1}. The treated sample was divided in two parts T1 and T2 for FT-IR analysis.

UV-Vis spectroscopic analysis

UV spectra of control and treated 2, 6-DAP samples were recorded on Shimadzu UV-2400 PC series spectrophotometer with 1 cm quartz cell and a slit width of 2.0 nm. The analysis was carried out using wavelength in the range of 200-400 nm. The treated sample was divided in two parts T1 and T2 for the analysis.

Results and Discussions

XRD study

XRD diffractogram of control and treated 2, 6-DAP are presented in the Figure 1. The XRD diffractogram of control 2, 6-DAP showed intense crystalline peaks at 2θ equals to 17.26°, 17.37°, 19.73°, 19.89°, and 22.63°. Whereas the treated 2, 6-DAP sample also showed similar crystalline nature. The XRD diffractogram of treated sample showed intense peaks at 2θ equals to 17.60°, 19.97°, 20.09°, 23.90°, and 29.59°. The comparative evaluation of the XRD diffractogram showed decrease in intensity of the treated 2, 6-DAP with respect to control (Figure 1). This showed that crystallinity of the 2, 6-DAP was decreased after biofield treatment as compared to control. It is assumed that biofield treatment may cause disturbance in molecular arrangement or long range pattern of the treated 2, 6-DAP that might leads to decrease in crystallinity.

The unit cell volume, crystallite size and change in molecular weight were computed from the XRD diffractogram and results are presented in Table 1. The unit cell volume of control 2, 6-DAP was 577.99 × 10^{-23} cm^3 and it was decreased to 560.77 × 10^{-23} cm^3 in treated sample. The treated 2, 6-DAP sample showed 2.97% decrease in unit cell volume as compared to control sample. Whereas the molecular weight of control 2, 6-DAP was 113.14 g/mol; however it was decreased to 109.77 g/mol in treated sample. The molecular weight was decreased by 2.98%

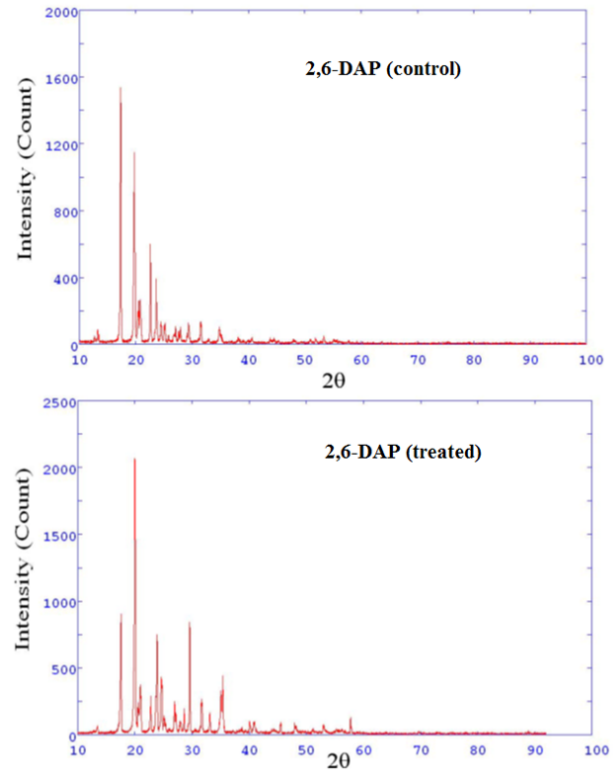

Figure 1: XRD diffractogram of control and treated 2, 6-Diaminopyridine.

Compound Characteristics	Control	Treated	% change
Unit cell volume (10^{-23} cm^3)	577.99	560.77	-2.97
Molecular Weight (g/mol)	113.14	109.77	-2.98

Table 1: XRD data (unit cell volume, crystallite size and molecular weight) of control and treated 2, 6-Dimanopyridine.

in treated 2, 6-DAP as compared to control. It is hypothesized that biofield energy may be acted on treated 2, 6-DAP crystals at nuclear level and altered the number of proton and neutrons as compared to control, which may lead to change in its molecular weight [27].

The crystallite size was calculated using Scherer formula and data are reported in Figure 2. The crystallite size of control 2, 6-DAP was 139.48 nm and it was decreased to 105.02 nm in treated sample. The result showed reduction in crystallite size by 24.70% in treated 2, 6-DAP with respect to control. The decrease in crystallite size in treated 2, 6-DAP was may be due to development of internal strain in the compound that led to reduction in crystallite size in the sample (Figure 2). Zhang et al. reported that presence of internal strains and increase of atomic displacement from their ideal lattice positions cause reduction in crystallite size [28]. Hence, it is assumed that biofield treatment may induce internal strain, which may decrease the crystallite size of the 2, 6-DAP as compared to control. It was previously suggested that Nano scale particle size and small crystallite size can overcome slow diffusion rate by reducing overall diffusion distance and this enhances the net reaction rate [29,30]. Hence, it is assumed that lower crystallite size of treated 2, 6-DAP may improve its reaction rate [31] and it could be utilized as intermediate for synthesis of pharmaceutical compounds.

DSC Study

DSC thermo gram of control and treated 2, 6-DAP are depicted in Figure 3. DSC thermogram of control 2, 6-DAP showed two endothermic peak behaviors in the sample. The first endothermic inflexion was observed at 74.26°C corresponded to melting of the monomeric form of control 2, 6-DAP. The second endothermic peak was observed at 122.34°C corresponded to melting of dimeric form of control 2, 6-DAP, that was in agreement with reported melting point value in literature (115-123°C) [6]. Schwalbe et al. reported that 2, 6-DAP molecule has two monomer and dimmer forms [4]. They suggested that presence of hydrogen bonds in dimer lattice form increased its melting point with respect to monomer form. Likewise, the DSC thermogram of treated 2, 6-DAP also showed occurrence of two endothermic peaks. The first peak was observed at around 78°C, which was due to melting of monomeric form in treated sample (Figure 3). The second endothermic peak was observed at 122.80°C corresponded to melting of the dimer form of the compound.

The latent heat of fusion was computed from the respective DSC thermogram of control and treated 2, 6-DAP samples and data are presented in Table 2. The control 2, 6-DAP showed a latent heat of fusion of 109.5 J/g; however, it was increased considerably in the treated 2, 6-DAP (148.18 J/g). The increase in latent heat of fusion in the treated 2, 6-DAP was 35.32% that showed significant increase as compared to control 2, 6-DAP. It was reported that intermolecular forces exist between molecules of a material, hence, energy required to overcome this interaction is known as latent heat of fusion. Hence, the energy absorbed during phase change of a material from solid to liquid is stored as potential energy in the substance [32]. Thus, it is assumed that biofield treatment may enhance the potential energy of the treated 2, 6-DAP that may lead increase in latent heat of fusion of sample with respect to control.

TGA study

TGA thermogram of control and treated 2, 6-DAP are presented in Figure 4. The TGA thermogram of control 2, 6-DAP showed one step thermal degradation pattern. The sample started to degrade at around 148°C and the thermal degradation was terminated at 225°C. During this step sample lost 69.07% of its weight. However, the treated

reduction in weight loss with respect to control revealed the increase in thermal stability of the sample

Particle size and surface area analysis

Particle size (d_{50} and d_{99}) of control and treated 2, 6-DAP are computed from the particle size distribution graph and results are presented in Figure 5. The d_{50} (average particle size) of control 2, 6-DAP was 88.59 µm and it was decreased to 70.47 µm in treated sample. Whereas, the d_{99} (size exhibited by 99% of the particles) of control 2, 6-DAP was 397.08 µm and it was decreased substantially to 169.32 µm in treated sample. The result showed significant decrease in d_{50} and d_{99} by 20.5 and 57.4% in treated 2, 6-DAP with respect to control sample (Figure 5). This marked reduction in particle size of treated 2, 6-DAP was may be due to energy milling caused by biofield treatment. The

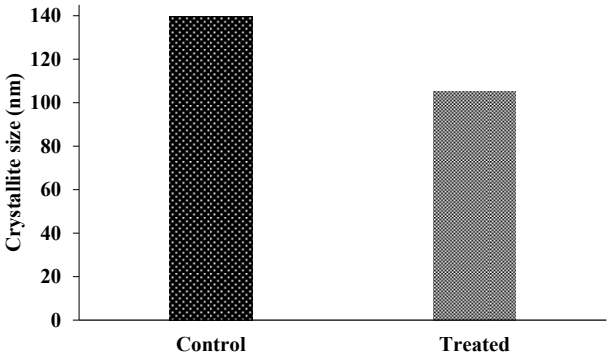

Figure 2: Crystallite size of control and treated 2, 6-Diaminopyridine.

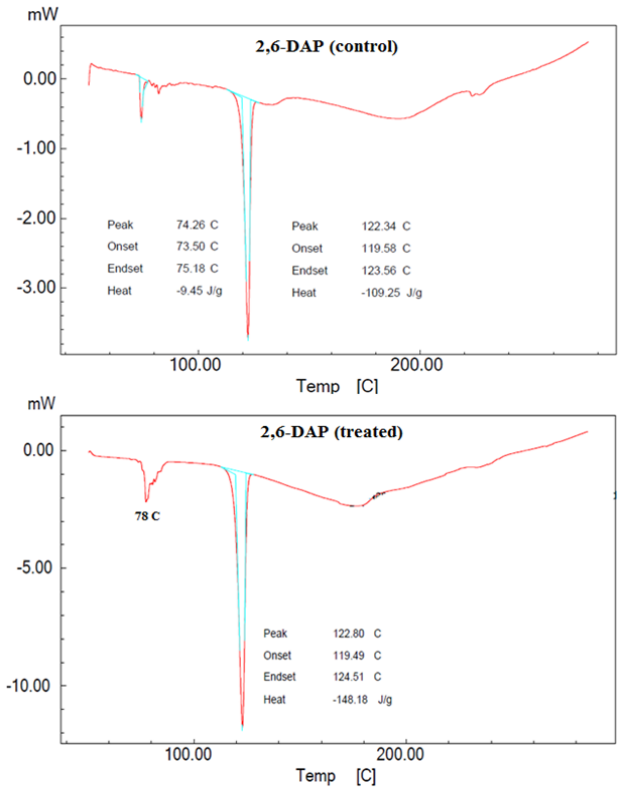

Figure 3: DSC thermogram of control and treated 2, 6-Diaminopyridine.

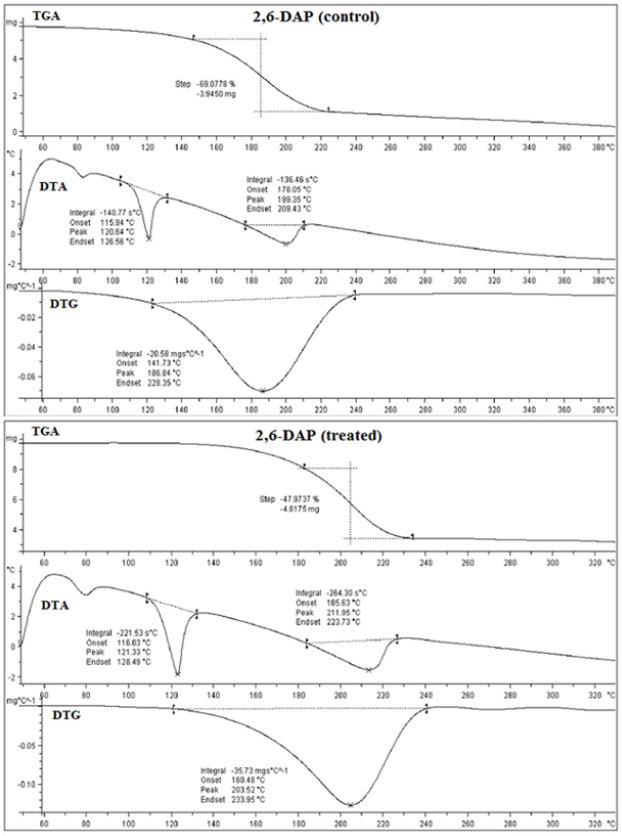

Figure 4: TGA thermogram of control and treated 2, 6-Diaminopyridine.

Parameter	Control	Treated
Latent heat of fusion ΔH (J/g)	109.5	148.18
Melting temperature (°C)	122.34	122.80
T_{max} (°C)	186.84	203.52
Weight loss (%)	69.07	47.97

Table 2: Thermal analysis data of control and treated 2, 6-Dimanopyridine.

2, 6-DAP started to degrade at around 184°C and this thermal event terminated at around 235°C. During this thermal process sample lost 47.97% of its weight. Hence, the result showed reduction in weight loss of treated 2, 6-DAP with respect to control.

DTA thermogram of control and treated 2, 6-DAP are presented in Figure 4. DTA thermogram of control 2, 6-DAP showed two endothermic peaks at 120.64°C and 199.35°C. The former peak was due to melting temperature of the control sample. Whereas, later peak was due thermal degradation of sample. DTA thermogram of treated 2, 6-DAP showed two endothermic peaks at 121.33°C due to melting temperature and second peak at 211.95°C which was may be due to thermal degradation of the sample. Hence, this showed increase in thermal degradation temperature of treated 2, 6-DAP with respect to control.

The maximum decomposition temperature (T_{max}) was evaluated from derivative thermogravimetry (DTG) of control and treated 2, 6-DAP. The DTG thermogram of control 2, 6-DAP showed a T_{max} at 186.84°C; however, it was significantly increased to 203.52°C in treated 2, 6-DAP. The significant increase in T_{max} of treated 2, 6-DAP and

energy milling led to fracture in the internal boundaries and that led to formation of smaller particles [27].

Surface area analysis was conducted using BET analysis and results are presented in Figure 6. The control 2, 6-DAP showed a surface area of 0.0594 m^2/g and it was increased to 0.1043 m^2/g in treated sample. The result showed significant increase in surface area by 75.58% in treated 2, 6-DAP as compared to control. Since the surface area and particle size changes are usually opposite to each other *i.e.*, smaller the particles size, larger the surface area and vice versa [33,34]. Hence, it is assumed that biofield treatment may cause reduction in particle size and increase in surface area of treated 2, 6-DAP with respect to control. It was reported that in a reaction between solid and liquid, the high surface area of the solid will ultimately affect the rate of reaction. Thus liquid and solid can bump into each other at the solid liquid interface, which is on the surface of the solid. Therefore more surface area of the solid will expose more molecules to the liquid, which allows for a faster reaction [35]. Thus, increase in surface area might improve solubility of treated 2, 6-DAP that could improve its reaction rate during synthesis of pharmaceutical compounds.

FT-IR spectroscopy

FT-IR spectroscopy was used to investigate the structural changes in the treated 2, 6-DAP with respect to control. FT-IR spectrum of control and treated 2, 6-DAP are presented in Figure 7. FT-IR spectrum of control 2, 6-DAP showed characteristic vibration peaks at 3390, 3309 and 3132 cm^{-1} due to N-H asymmetric, N-H symmetric and N^+-H stretching vibrations, respectively. Vibration peaks at 2951, and 2883 cm^{-1} were due to C-H aromatic and C-H symmetric stretching (methyl), respectively. FT-IR peak at 1637 cm^{-1} was due to bending vibrations of N-H group of pyridine. The vibration peaks for C=C, C-N stretching and C-H in plane bending were observed at 1577, 1184, and 1120 cm^{-1}, respectively. Vibration peaks at C-O stretching was noticed at 1064 cm^{-1}. FT-IR results were well supported from the published literature [34].

FT-IR spectrum of 2, 6-DAP (T1) is presented in Figure 7. The FT-IR spectrum showed peaks at 3390, 3306 and 3126 cm^{-1} corresponded to N-H asymmetric, N-H symmetric and N^+-H stretching vibrations. The other typical peaks observed at 2951, and 2756 cm^{-1} were due to C-H aromatic and C-H symmetrical vibrations, respectively. Vibration peaks for N-H bending and C=C group stretching were observed at 1637 and 1577 cm^{-1}, respectively. FT-IR peaks at 1182, and 1064 cm^{-1} corresponded to C-N and C-O, stretching vibrations. C-H out of plane bending vibration was observed at 1118 cm^{-1}.

FT-IR spectrum of 2, 6-DAP (T2) is shown in Figure 7. The FT-IR spectrum showed peaks at 3377, 3302 and 3138 cm^{-1} corresponded to N-H asymmetric, N-H symmetric and N^+-H stretching vibrations, respectively. C-H (aromatic) and C-H methyl stretching were observed at 2949 and 2798 cm^{-1}, respectively. FT-IR peaks at 1604, 1589, and 1184 cm^{-1} were mainly due to N-H bending, and C=C, C-N stretching vibrations. Vibration bands at 1116 and 1064 cm^{-1} were corresponded to C-H out of plane bending and C-O stretching vibrations. Overall, the result showed changes in O-H stretching (3390→3377 cm^{-1}), C-H stretching (3132→3138 cm^{-1}) and N-H bending (1637→1604 cm^{-1}) FT-IR peaks with respect to control. The downward shift of O-H stretch and N-H bending of 2, 6-DAP (T2) could be due to biofield treatment. It is presumed that decrease in wavenumber of these FT-IR peak may be due to decrease in force constant and bond strength of treated 2, 6-DAP (T2) as compared to control [35].

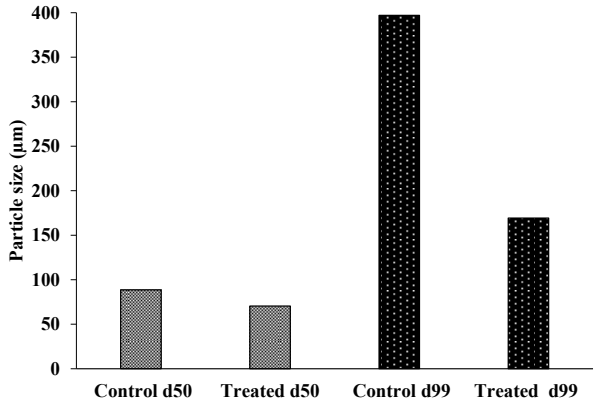

Figure 5: Particle size (d_{50} and d_{99}) data of control and treated 2, 6-Diaminopyridine.

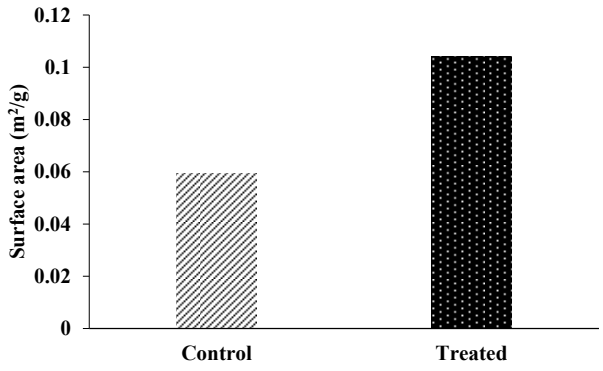

Figure 6: Surface area of control and treated 2, 6- Diaminopyridine.

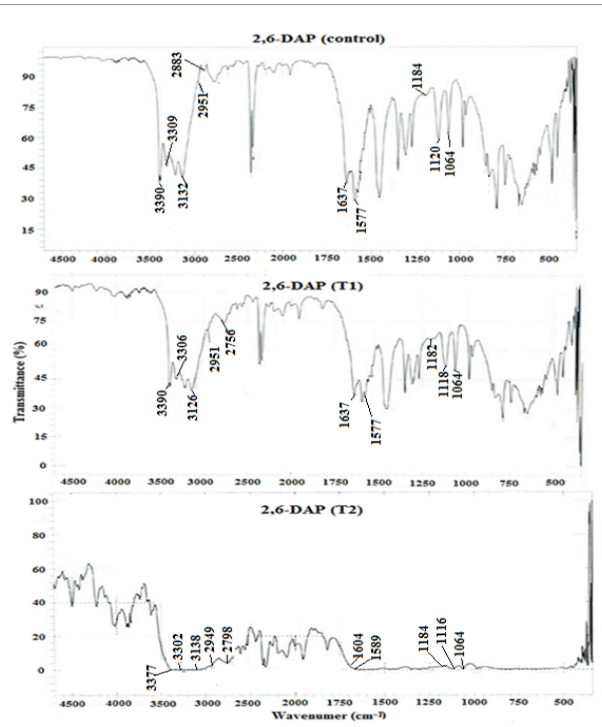

Figure 7: FT-IR spectra of control and treated 2, 6- Diaminopyridine (T1 and T2).

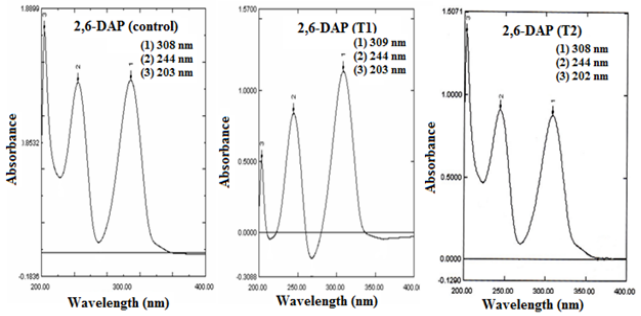

Figure 8: UV-visible spectra of control and treated 2, 6-Diaminopyridine (T1 and T2).

UV visible spectroscopy

UV-visible spectroscopy was used to investigate the chemical changes in treated 2, 6-DAP with respect to control. UV visible spectra of control and treated sample are shown in Figure 8. The UV spectrum of control 2, 6-DAP showed absorption peaks at 308, 244, and 203 nm (λ_{max}). However, the treated 2, 6-DAP (T1) showed absorption peaks at 309, 244, and 203 nm (λ_{max}). Likewise the 2, 6-DAP (T2) also showed similar absorption peaks at 308, 244 and 202 nm (λ_{max}). The result showed no alterations in absorption peaks of the treated 2, 6-DAP as compared to control sample.

Conclusion

XRD analysis showed reduction in peak intensity of treated 2, 6-DAP with respect to control that may be due to decrease in crystallinity of the sample. XRD results showed decrease in unit cell volume and molecular weight in treated 2, 6-DAP sample with respect to control. A significant decrease in crystallite size of treated 2, 6-DAP was observed as compared to control. DSC analysis showed no significant change in the melting temperature of treated 2, 6-DAP with respect to control. However, significant increase in latent heat of fusion was evidenced in treated 2, 6-DAP with respect to control. TGA analysis of treated 2, 6-DAP showed reduction in weight loss as compared to control. The treated 2, 6-DAP showed increase in T_{max} with respect to control. This showed the increase in thermal stability of the treated 2, 6-DAP with respect to control. Moreover, the treated sample showed substantial reduction in particle size as compared to control. Additionally, significant increase in surface area was observed in treated 2, 6-DAP with respect to control. FT-IR analysis showed changes in O-H stretching, C-H stretching and N-H bending with respect to control. However, UV-visible analysis results of treated compound showed no alteration in absorption peaks when compared to control. Altogether, the results demonstrated the substantial impact of biofield treatment on physical, thermal and spectral properties of treated 2, 6-DAP. It is assumed that high thermal stability of treated 2, 6-DAP could be used as intermediate for synthesis of pharmaceutical compounds.

Acknowledgements

We thank Dr. Cheng Dong of NLSC, institute of physics, and Chinese academy of sciences for permitting us to use Powder X software for analyzing XRD results. The authors would also like to thank Trivedi Science, Trivedi Master Wellness and Trivedi Testimonials for their support during the work.

References

1. Horn AS, Gaston S (1984) 2, 4-Diaminopyridine as a pharmacologic agent. US4562196.
2. Judge S, Bever CT Jr (2006) Potassium channel blockers in multiple sclerosis: neuronal Kv channels and effects of symptomatic treatment. Pharmacol Ther 111: 224-259.
3. Naixing W, Boren C, Yuxiang O (1993) Synthesis of N-2,4,6-trinitrophenyl-N'-2,4,dinitrobenzofuroxano-3,5-dinitro-,G-diaminopyridine. J Energ Mater 11: 47-50.
4. Schwalbe CH, Williams GJB, Koetzle TF (1987) A neutron diffraction study of 2, 6-Diaminopyridine at 20K. Acta Cryst C 43: 2191-2195.
5. Mohammadi H, Hassanzadeh A, Khodabakhsh R (2010) The effect of fast neutron and gamma irradiation on thermal, structural and colorant properties of 2, 6-diaminopyridine. Appl Radiat Isot 68: 1884-1891.
6. Trivedi MK, Patil S, Tallapragada RM (2013) Effect of biofield treatment on the physical and thermal characteristics of vanadium pentoxide powders. J Material Sci Eng S11: 001.
7. Trivedi MK, Patil S, Tallapragada RM (2013) Effect of biofield treatment on the physical and thermal characteristics of silicon, tin and lead powders. J Material Sci Eng 2: 125.
8. Trivedi MK, Patil S, Tallapragada RM (2014) Atomic, crystalline and powder characteristics of treated zirconia and silica powders. J Material Sci Eng 3: 144.
9. Trivedi MK, Patil S, Tallapragada RMR (2015) Effect of biofield treatment on the physical and thermal characteristics of aluminum powders. Ind Eng Manag 4: 151.
10. Myers, Richard (2003) The basics of chemistry. Westport, Connecticut, Greenwood Press.
11. Korotkov K (2002) Human Energy Field: study with GDV bioelectrography. Backbone publishing, New York.
12. Becker RO, Selden G (1985) The body electric: electromagnetism and the foundation of life, William Morrow and Company, New York City.
13. Barnes RB (1963) Thermography of the human body. Science 140: 870-877.
14. Born M (1971) The Born-Einstein Letters. (1stedn), Walker and Company, New York.
15. Cohen S, Popp FA (2003) Bio photon emission of the human body. Indian J Exp Biol 41: 440-445.
16. Rubik B (2002) The biofield hypothesis: its biophysical basis and role in medicine. J Altern Complement Med 8: 703-717.
17. Baldwin AL, Hammerschlag R (2014) Biofield-based therapies: a systematic review of physiological effects on practitioners during healing. Explore (NY) 10: 150-161.
18. Shinde V, Sances F, Patil S, Spence A (2012) Impact of biofield treatment on growth and yield of lettuce and tomato. Aust J Basic Appl Sci 6: 100-105.
19. Sances F, Flora E, Patil S, Spence A, Shinde V (2013) Impact of biofield treatment on ginseng and organic blueberry yield. Agrivita J Agric Sci 35: 22-29.
20. Lenssen AW (2013) Biofield and fungicide seed treatment influences on soybean productivity, seed quality and weed community. Agricultural Journal 8: 138-143.
21. Patil SA, Nayak GB, Barve SS, Tembe RP, Khan RR (2012) Impact of biofield treatment on growth and anatomical characteristics of *Pogostemon cablin* (Benth.). Biotechnology 11: 154-162.
22. Trivedi MK, Patil S (2008) Impact of an external energy on *Staphylococcus epidermis* [ATCC –13518] in relation to antibiotic susceptibility and biochemical reactions – An experimental study. J Accord Integr Med 4: 230-235.
23. Trivedi MK, Patil S (2008) Impact of an external energy on *Yersinia enterocolitica* [ATCC –23715] in relation to antibiotic susceptibility and biochemical reactions: An experimental study. Internet J Alternative Med 6: 2.

24. Trivedi MK, Bhardwaj Y, Patil S, Shettigar H, Bulbule A (2009) Impact of an external energy on *Enterococcus faecalis* [ATCC – 51299] in relation to antibiotic susceptibility and biochemical reactions – An experimental study. J Accord Integr Med 5: 119-130.

25. Nayak G, Altekar N (2015) Effect of biofield treatment on plant growth and adaptation. J Environ Health Sci 1: 1-9.

26. Trivedi MK, Nayak G, Patil S, Tallapragada RM, Latiyal O (2015) Studies of the atomic and crystalline characteristics of ceramic oxide nano powders after bio field treatment. Ind Eng Manage 4: 161.

27. Zhang K, Alexandrov IV, Kilmametov AR, Valiev RZ, Lu K (1997) The crystallite-size dependence of structural parameters in pure ultrafine-grained copper. J Phys D Appl Phys 30: 3008-3015.

28. Chaudhary AL, Sheppard DA, Paskevicius M, Webb CJ, Gray EM, et al. (2014) Mg_2Si nanoparticle synthesis for high pressure hydrogenation. J Phys Chem C 118: 1240-1247.

29. Chaudhary AL, Sheppard DA, Paskevicius M, Saunders M, Buckley CE (2014) Mechanochemical synthesis of amorphous silicon nanoparticles. R Soc Chem Adv 42: 21979-21983.

30. Chaudhary AL, Sheppard DA, Paskevicius M, Pistidda, C, Dornheim M, et al. (2015) Reaction kinetic behavior with relation to crystallite/grain size dependency in the Mg–Si–H system. Acta Mater 95: 244-253.

31. Moore J (2010) Chemistry: The molecular science. (4thedn) Brooks Cole.

32. Mennucci B, Martinez JM (2005) How to model solvation of peptides? Insights from a quantum-mechanical and molecular dynamics study of N-methylacetamide. I. Geometries, infrared, and ultraviolet spectra in water. J Phys Chem B 109: 9818-9829.

33. Bendz D, Tuchsen PL, Christensen TH (2007) The dissolution kinetics of major elements in municipal solid waste incineration bottom ash particles. J Contam Hydrol 94: 178-194.

34. Murugesan V, Saravanabhavan M, Sekar M (2015) Synthesis, spectroscopic characterization and structural investigation of a new charge transfer complex of 2, 6-diaminopyridine with 4-nitrophenylacetic acid: Antimicrobial, DNA binding/cleavage and antioxidant studies. Spectrochim Acta 147: 99-106.

35. Pavia DL, Lampman GM, Kriz GS (2001) Introduction to spectroscopy. (3rd edn), Thomson learning, Singapore.